Layering Transitions and Dynamics of Confined Liquid Films

Jianping Gao, W. D. Luedtke, and Uzi Landman

School of Physics, Georgia Institute of Technology, Atlanta, Georgia 30332

Using grand-canonical molecular dynamics simulations and free energy calculations of spherical molecular confined films, we investigate the internal energy and entropic origins of density layering and solvation force oscillations. We show that these properties, as well as diffusion and rheological characteristics of such films, depend on interfacial commensurability, with commensurate films exhibiting abrupt solidification for relatively thick, 5 or 6 layer, films.   [S0031-9007(97)03672-7]

A central property of liquids confined between solid boundaries which are smooth on the molecular scale (as well as of films adsorbed on a solid surface) is their tendency to organize into layered structures [1,2], where the mean local density of the liquid oscillates with distance normal to the boundaries. This property is portrayed as oscillatory solvation forces between confining surfaces [1] (that is, oscillations in the force between the confining boundaries as the distance between them, i.e., the confining gap width, is varied, with a period approximately equal to the width of the film molecules), which were observed and simulated for simple liquids (e.g., modeled as spheres [2–4]) and nonpolar globular molecules [1,5–8] (e.g., octamethylcyclotetrasiloxane, OMCTS), as well as for complex liquids such as straight-chain alkanes (e.g., *n*-hexadecane [1,9–12], $n\text{-}C_{16}H_{34}$, and tetracocane [12], $n\text{-}C_{24}H_{50}$) and polar liquids (e.g., water [1,13]).

Furthermore, confined ultrathin films may exhibit different responses [14] (in shear [14], as well as in response to variation of the normal distance between the confining surfaces [7]): a liquidlike response in which the liquid responds to the deformation by flow, or spreading (as in drainage measurements [15,16]), and a solidlike response characterized by observation of the development of "yield stress" in the confined fluid [17]. Most pertinent to our study are recent surface force apparatus (SFA) measurements [7] on confined films of OMCTS (whose diameter is ∼9 Å), suggesting the abrupt development of solidlike behavior in relatively thick films of 6 layers, induced solely by the increased confinement (i.e., without an imposed lateral motion of the confining surfaces), although there is some debate concerning the nature of the transition [8].

While layering of confined films and solvation force oscillations are related, the distinction between these two phenomena should be emphasized [1]. As discussed by us recently [11,12], the strong attenuation of force oscillations in squalane films (a branched alkane, 2,6,10,15,19,23-hexamethyl-tetracosane) in comparison to those found for films of globular molecules and straight-chain alkanes (*n*-hexadecane and *n*-tetracosane) is not correlated with reduced layering in the branched molecular films. Rather, the difference in solvation force characteristics between the branched and straight-chain (as well as globular) molecular

films originates from different modes of response in these systems to variation of the degree of the confinement, with the former exhibiting liquidlike characteristics.

In this study we show, using a recently developed grand-canonical molecular dynamics (GCMD) method [11], that underlying the solvation forces in confined films are the combined contributions to the free energy from entropic and internal energy terms, and their variations with the degrees of confinement [1,12]. Moreover, we demonstrate, through simulations of spherical molecules, that the solvation force oscillations and rheological properties of such confined films depend on the commensurability between the surface structure of the confining solids and the liquid molecules, with commensurate films showing a rather abrupt transition from liquidlike to solidlike response characteristics for relatively thick (≲6 layers) films [7].

The simulations were performed in the constant chemical potential (μ), pressure (P), and temperature (T) ensemble (μ, P, T), using the GCMD. In this method [11], which models the configuration used in SFA and tip-based experiments, the simulation cell contains both liquid molecules and solid blocks, with periodic boundary conditions replicating the cell in all three directions. The solid blocks, which are immersed in the liquid, are of finite size in the x and z directions, with the distance between the two solid surfaces in the z direction defining the width of the gap (D) confining the fluid [in our simulations the solid surfaces forming the gap in the middle of the cell are modeled as (111) planes of a face-centered cubic (fcc) solid]. In the y direction, the solid blocks are extended through the whole cell, with the rest of the space in this three-dimensional cell filled with fluid molecules. The size of the cell in the x direction, H_x, is taken to be sufficiently large so that the molecules in the regions outside the confined one, and in equilibrium with it, can exhibit bulk liquid behavior. H_x is allowed to vary dynamically, using constant pressure MD, from ∼135 to ∼210 Å, depending on the gap width D. The hydrostatic pressure, determining the magnitude of H_x, is taken to be 1 atm. The extent of the immersed solid blocks in the x direction is ∼15 Å and the height of each block is $d_s = 15$ Å; the size of the cell in the z direction H_z is thus given by $H_z = 2d_s + D$ (D is varied between

~8–30 Å), and the size of the cell in the y direction is kept constant, $H_y \sim 40$ Å.

The fluid molecules were treated dynamically while the atoms of the solid substrates were static (treating the solids dynamically does not affect our results). The temperature of the system is controlled via scaling of the atomic velocities at infrequent intervals (when equilibrium is reached no temperature control is necessary); the temperature in the simulations was $k_B T = 0.835\epsilon$ (i.e., above the melting point of the bulk Lennard-Jones (LJ) material for $P = 1$ atm), where ϵ is the interatomic 6-12 LJ potential well depth; the intermolecular LJ parameters which we used are $\epsilon/k_B = 119.8$ K and $\sigma = 3.405$ Å, and for the interaction between the solid substrate atoms and the film molecules $\epsilon_{sf}/k_B = 2.4\epsilon$. Two systems were simulated: (i) a commensurate system (C) where the fcc substrate lattice constant $a = 5.798$ Å was chosen such that the solid and bulk liquids will have the same density [4], with $\sigma_{sf} = \sigma$, and (ii) an incommensurate system (IC), where $\sigma_{sf} = 3.021$ Å and the fcc lattice constant $a = 4.08$ Å (corresponding to that of gold). The initialization and equilibration procedures which we used were described by us previously [11,12]. We report results averaged (for each value of D) over ~ 100 ps ($\sim 10^4$ integration time steps using a Verlet algorithm), subsequent to prolonged equilibration periods (typically 200–600 ps).

The density profiles $\rho(z)$ for the C film, recorded versus distance in the direction normal to the surfaces, for a sequence of separations (gaps) between the confining surfaces is shown in Fig. 1. (See similar results for the IC case in Fig. 1 of Ref. [12].) In both cases these profiles show clear oscillatory patterns for $D \leq 26$ Å; for wider gaps a uniform (bulk) density distribution develops in the middle of the confined film, with layering near the two interfaces; see, e.g., $D = 28$ and 30 Å in Fig. 1.

Narrowing of the gap results in expulsion of molecules from the confined region ("squeezing out" of the film) and transition to a film with a smaller number of layers occurring with a periodicity of about 3.5 Å. Sharp, well-formed layered configurations (with similar layer densities) in the C film occur for a sequence of gap width (e.g., $D = 26, 22, 18, 15, 12$, and 9 Å, corresponding to 7, 6, 5, 4, 3, and 2 layers, respectively; see Fig. 1), with a lower degree of interlayer order for intermediate gap widths; in the IC film the well-formed layers occur for similar values [12].

Solvation forces $f_z(D)$ (i.e., the total force exerted by the interfacial film on the confining surfaces, which is the same as the force which would be required in order to hold the two surfaces at the corresponding separation) recorded during the approach of the two surfaces are shown for the C and IC systems in Fig. 2(a). The layering transitions in the confined films are portrayed in solvation force oscillations [Fig. 2(a)], with the local positive force maxima corresponding to configurations with well-formed layers, and the amplitudes of the force oscillations somewhat larger for the C film. In these configurations we find also a high de-
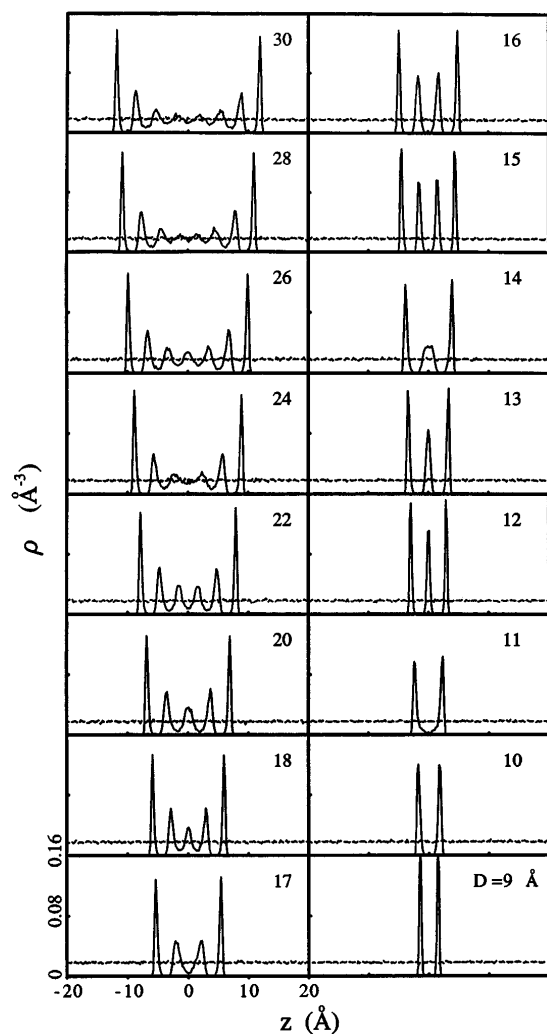

FIG. 1. Equilibrium density profiles for the commensurate film along the z direction (normal to the confining solid surfaces); solid lines correspond to the film in the confined region and the dashed lines calculated for the region outside the gap. The gap widths (D) for which the profiles were calculated are indicated. Note that the liquid density outside the confinement (dashed line) is uniform and remains constant for all values of D, while the layered density features in the confined film (particularly in the middle region of the film) vary in sharpness depending on the degree of confinement.

gree of intralayer order (hexagonally close-packed) which becomes sharper upon increased confinement [12], and is higher in the C film which is in epitaxy with the solid surfaces; the degree of intralayer order reduces for intermediate states between well-formed configurations.

Further insights into the layering transition processes are obtained from records of the number of molecules in the confined region, n_{cfn}, plotted versus the distance between the confining surfaces (D), shown in Fig. 2(c). The variation of n_{cfn} exhibits a steplike pattern with sharp drops in the number of confined molecules occurring for the transition from an n-layer film to an $(n - 1)$-layer one, with the steps becoming sharper as n decreases. (Note that the pattern extends for the C system to a larger value of D.)
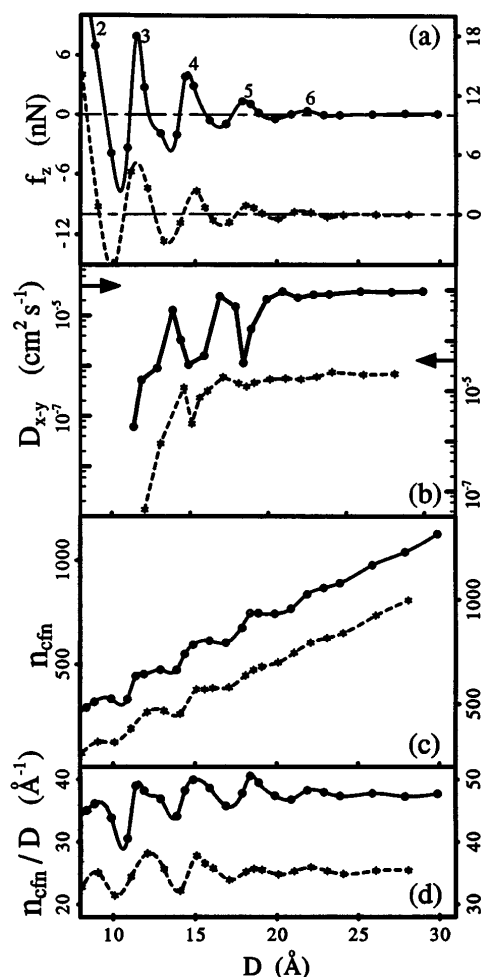
FIG. 2. (a) Equilibrium solvation forces f_z in nN plotted versus the width of the confining gap D in Å. (b) 2D diffusion constants D_{xy}, vs D plotted on a logarithmic scale. Simulated values in the bulk liquid are denoted by arrows. (c) Number of molecules in the confining gap, n_{cfn}, in (c), and n_{cfn}/D, in (d), plotted versus the gap width D in Å. Results are for the C (solid line) and IC (dashed) confined LJ films, with the left and right ordinate, respectively.

For each of these transitions the drop in n_{cfn} is caused by a relatively small reduction ($\sim 0.5-1$ Å) of the gap width from that corresponding to an initial well-layered configuration of the film [i.e., the number of layers in the film at the bottom of each step is decreased by one from that corresponding to the film at the top of the step (and the plateau)].

Plots of n_{cfn}/D versus D [see Fig. 2(d) where n_{cfn}/D is proportional to the number density of molecules in the gap] suggest that below a certain thickness (~ 6 layers in the C system, and 4 to 5 layers in the IC one) the films exhibit certain features characteristic of the solidlike response; that is, when the confining gap width is slightly reduced (typically $\Delta D \sim 1$ Å), starting from one of the well-formed layered configurations of the film with n_L layers [corresponding to the maxima in the solvation force shown in Fig. 2(a)], the film "yields" through expulsion of approximately a layer's worth of molecules into the surrounding

liquid, causing a sharp decrease in the confined film density. During further reduction of the gap width, the number of confined molecules remains almost constant [plateaus of n_{ncf}, Fig. 2(c)], with an associated increase of the confined film density [Fig. 2(d)] which is accompanied by enhancement of the order in the film. This process continues until a gap width corresponding to a maximally ordered layered film (with $n_L - 1$ layers) is reached, for which the confined film density maximizes. This sequence of events repeats with a period of ~ 3.5 Å.

Additional evidence for a confinement induced transition of the film to a solidlike regime is provided by the 2D diffusion constant D_{xy} (i.e., parallel to the confining surfaces), calculated as the slope of the squared displacements of particles as a function of time, and plotted versus the gap width [Fig. 2(b)]. Since the interfacial layers of the film in direct contact with substrates show insignificant diffusion they were not included in the calculations. In all cases the D_{xy} values calculated for the second layers of the films are the same as those for the whole films. For the C system D_{xy} undergoes an abrupt decrease upon transition from a 6- to a 5-layer film, and similarly for the 5-to-4–layer and 4-to-3–layer transitions. The local maxima of D_{xy} for gap width between the well-formed layered states of the film correspond to the intermediate expulsion-disordering stages. We also note that a similar behavior, though of lesser magnitude, occurs also for the IC film, starting with the 5-to-4–layer transition. The difference between the C and IC systems correlates with the smaller degree of in-layer order in the latter one.

Furthermore, shearing the 5- and 4-layer C system at a constant velocity of 0.5 m/s (by translating the confining blocks in opposite directions parallel to the y axis for which the confining solid blocks extend over the entire periodically replicated cell) resulted in the development of an internal stress in the film (in the directions opposite to the shear) growing linearly with the imposed strain, until a critical value is reached beyond which the film yields. Stopping the relative motion of the confining solid surfaces prior to yielding (for strain values of 0.055 and 0.068 for the 5- and 4-layer films, respectively), the deformed C films maintained the stored induced internal stress (13.4 and 42.6 MPa, respectively), which is the signature of solidlike behavior; the calculated corresponding shear moduli of the 5- and 4-layer films are 250 and 626 MPa, respectively, which are close to typical LJ solid values. In contrast, for the IC system under shear the incommensurability of the film-surface interface causes boundary slip with insignificant accumulation of internal stress in the film. The above diffusion and shear-response characteristic of the C film correlate with recent SFA measurements on OMCTS films [7], where a rather abrupt transition into a solidlike state has been reported for a 6-layer thick film.

We return now to a brief discussion of the entropic and energetic origins of the solvation forces [12]. The change in the free energy of the confined liquid associated with a

change of the gap size from D_0 to D, performed quasistatically under isothermal conditions and for a constant number of confined molecules, is equal to the reversible work done in this process, i.e., $\Delta F(D, D_0) = -\int_{D_0}^{D} f_z(z') \, dz'$. From the definition of ΔF, i.e., $\Delta F(D, D_0) = \Delta U - T\Delta S$, where ΔU and ΔS are the corresponding changes in the internal energy and entropy of the confined system, one can determine the entropic contribution $T\Delta S$, by evaluating $\Delta F(D, D_0)$ and the internal energy changes from the MD simulation. In $\Delta F(D, D_0)$ the pressure-volume contribution $P\Delta V$ has been omitted since both P and ΔV are small. Results for ΔU, $T\Delta S$, and ΔF, calculated for the simulated C system (with the extensive properties scaled to a constant number of confined molecules [12]) are shown in Fig. 3(a) (results for the IC case can be found in Ref. [12]). The main features noted from these results are the oscillations in the free energy [which are phase shifted when compared to the solvation force oscillations; i.e., the extremal values of $\Delta F(D)$ correspond to zeros of $f_z(D)$], and the nearly monotonic variations of the internal energy and entropic contribution. We note here that the development of well-formed layered configurations starts at gap widths corresponding to the minima of ΔF, sharpening further as the solvation forces achieve their maximal values.

The internal energy and entropic contributions to the total solvation force $f_z(D)$ can be now evaluated as $f_z^{(U)}(D) = -\partial(\Delta U)/\partial D$ and $f_z^{(S)}(D) = \partial(T\Delta S)/\partial D$, which when combined yield the total solvation force $f_z(D) = -\partial(\Delta F)/\partial D$. The results displayed in Fig. 3(b) show that both the internal and entropic contributions

to the solvation force exhibit oscillations as a function of the width of the confining gap. However, while the entropic contribution to the solvation force is overall repulsive (positive values) showing local maxima in the vicinity of the well-layered configurations, the internal energy contribution is overall attractive (negative values), reflecting the nature and degree of molecular organization and ordering during the squeezing process.

These results pertaining to the dependencies of the structural, dynamical, rheological, and response properties of confined films on interfacial commensurability, and on molecular structure [11,12] (that is, globular, straight, and branched chain molecules) suggest further systematic SFA and tip-based experiments aimed at probing these phenomena, and, in particular, the nature of transitions from liquidlike to solidlike behavior which are currently a source of experimental controversy [7,8].

[1] J. N. Israelachvili, *Intermolecular and Surface Forces* (Academic Press, New York, 1992), 2nd ed.
[2] For a recent review, see B. Bhushan, J. N. Israelachvili, and U. Landman, Nature (London) **374**, 607 (1995).
[3] (a) C. L. Rhykerd, Jr., M. S. Schoen, D. Diester, and J. Cushman, Nature (London) **330**, 461 (1987); (b) see citations 38–41 cited in Ref. [2].
[4] P. A. Thompson and M. O. Robbins, Science **250**, 792 (1990).
[5] J. N. Israelachvili and R. G. Horn, J. Chem. Phys. **35**, 1400 (1981).
[6] S. Granick, A. L. Demirel, L. L. Cai, and J. Peanasky, Isr. J. Chem. **35**, 75 (1995).
[7] J. Klein and E. Kumacheva, Science **269**, 816 (1995).
[8] A. L. Demirel and S. Granick, Phys. Rev. Lett. **77**, 2261 (1996).
[9] H. K. Christenson, D. W. R. Gruen, R. G. Horn, and J. N. Israelachvili, J. Chem. Phys. **87**, 1834 (1987).
[10] (a) U. Landman, W. D. Luedtke, J. Ouyang, and T. K. Xia, Jpn. J. Appl. Phys. **32**, 1444 (1993); (b) W. D. Luedtke and U. Landman, Comput. Mater. Sci. **1**, 1 (1992).
[11] J. Gao, W. D. Luedtke, and U. Landman, J. Chem. Phys. **106**, 4309 (1997).
[12] J. Gao, W. D. Luedtke, and U. Landman, J. Phys. Chem. B **101**, 4013 (1997).
[13] S. J. O'Shea, M. E. Welland, and J. B. Pethica, Chem. Phys. Lett. **223**, 336 (1994); J. P. Cleveland, T. E. Schaffer, and P. K. Hansma, Phys. Rev. B **52**, R8692 (1995).
[14] S. Granick, Science **253**, 1374 (1991).
[15] D. Y. C. Chan and R. G. Horn, J. Chem. Phys. **83**, 5311 (1985).
[16] J. N. Israelachvili, J. Colloid Interface Sci. **110**, 263 (1986).
[17] G. Reiter, A. L. Demirel, and S. Granick, Science **263**, 1741 (1994).
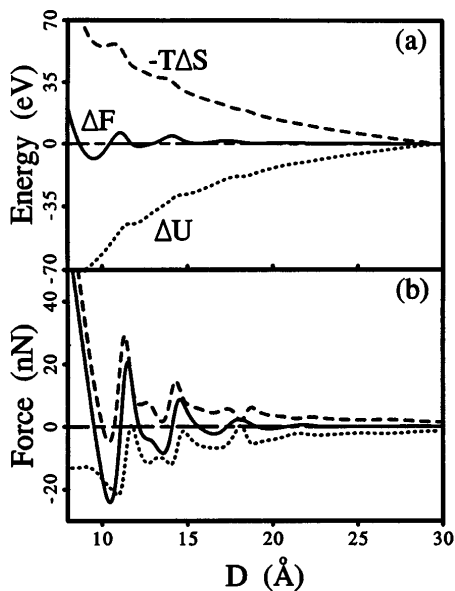
FIG. 3.   Variation with D of the total free energy ΔF (a) and force (b), and the internal energy (dotted) and entropy (dashed) contributions, calculated for the C film. All displayed properties were scaled to a constant number of molecules in the confinement; see Ref. [12]. Energies, forces, and distances in units of eV, *nN*, and Å, respectively.